Hindawi
Journal of Advanced Transportation
Volume 2022, Article ID 5274056, 11 pages
https://doi.org/10.1155/2022/5274056

Research Article

Car-Following Dynamics, Characteristics, and Model Based on Interaction Potential Function

Dayi Qu, Zixu Zhao, Chunyan Hu, Tao Wang, and Hui Song

School of Mechanical and Automotive Engineering, Qingdao University of Technology, Qingdao, China

Correspondence should be addressed to Zixu Zhao; resolution0219@163.com

Received 24 October 2021; Revised 12 December 2021; Accepted 10 January 2022; Published 29 January 2022

Academic Editor: Sara Moridpour

To model the car-following behavior more accurately, we carried out the molecular similarity analysis between the vehicles on the road and the inert gas system, comparing vehicles with microscopic particles in long and narrow pipes. The complex car-following interaction behavior is simplified into a dynamic process of the follower car that is constantly seeking to maintain the required safety distance from the leading vehicle. Through mathematical derivation of the Lennard–Jones potential function suitable for thermodynamic analysis of inert gas systems, the influence of each variable on the potential energy is clarified, and the existing problems of the existing molecular car-following model are analyzed, referring to the general Lennard–Jones potential function to build the vehicle interaction potential function. Considering the impact of the road wall potential generated by the lane boundary, a car-following model based on Lennard–Jones interaction potential is presented. The simulation test results show that compared with the existing molecular car-following model and IDM model, the average absolute error and root mean square error of the vehicle acceleration results obtained by this model and the actual data are lower, which proves that the vehicle is based on the Lennard–Jones interaction potential. The vehicle-following model based on Lennard–Jones interaction potential has a better fitting effect on the real vehicle-following behavior.

1. Introduction

Vehicle-following behavior is the basic element of micro-traffic flow characteristics, and the research on it has been the focus of transportation discipline since the 1950s. After a lot of research, domestic and foreign scholars have constructed a series of mathematical models to describe the motion state of the vehicle-following behavior, among which the classical models are the stimulus-response model, psychological-physiological model, neural network model, and safety distance model. Gazis et al. [1] presented the GM model expression based on the linear car-following model, also known as the GHR model. Bando [2] proposes an optimized speed car-following model from the perspective of statistical physics. Helbing and Tilch [3] considered the influence of speed difference on the acceleration of car-following cars and presented a generalized force (GF) model. Jiang et al. [4] considered the influence of the negative speed difference and the positive speed difference on the acceleration of the car-following and presented a full velocity difference (FVD) model.

Traditional car-car following models based on a kinematic relationship mostly consider such factors as vehicle-vehicle interaction distance and speed. In recent years, some scholars have compared the dynamic characteristics of vehicles in the road with those of microparticles to study the car-following behavior. Chen [5] studied the application of molecular dynamic methods to analyze the car-following characteristics and traffic flow stability. Qu et al. [6] built a molecular dynamics model of car-following based on the molecular dynamics analysis of the car-following behavior.

Later, some scholars began to try to treat vehicle interaction as a potential energy field to study the interaction between vehicles [7]. Li et al. [8] used the safe potential field theory to build a car-following model in a networked environment. Li et al. [9] built a molecular dynamics-based car-following model based on the vehicle-following molecular dynamics model using the presented vehicle interaction potential. Yang et al.

[10] considered the influence of the speed of the preceding vehicle and improved this model. The car-following model based on molecular dynamics and its improved model use the Lennard–Jones 6–12 potential function to study the car-following behavior, while the Lennard–Jones 6–12 potential function is essentially a potential function applicable to the thermodynamics of microparticles in fluids. Its applicability and rationality in describing the car-following behavior in the macroworld remain to be discussed.

Therefore, this study considers the differences of motion conditions between the microparticles and the vehicle, deeply analyses the similar relationship between the microparticles and vehicle interaction, builds a potential function more suitable for reflecting the vehicle-following behavior, and establishes the corresponding vehicle-following dynamic model.

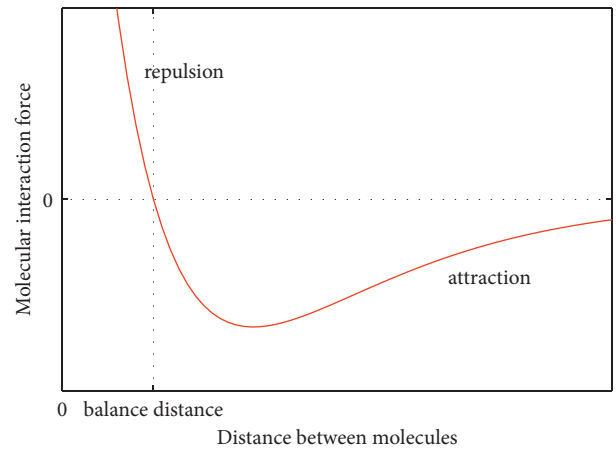

Figure 1: The molecular spacing and their interaction.

2. System Similarity Analysis

In the inert gas system, the intermolecular force generally considers the Van der Waals force alone. Under this action, there are forces of mutual attraction and repulsion between the molecules. According to the different relationship between the molecular distance r and the equilibrium distance r_0, the characteristics of the force shown are different, which can be divided into the following four situations:

(1) $r \gg r_0$: molecular spacing is much larger than the equilibrium distance, and there is almost no interaction between the molecules

(2) $r > r_0$, and $r - r_0 < \xi$: when the molecular spacing is greater than the equilibrium distance and within a certain range, the intermolecular attraction is obvious

(3) $r < r_0$: the molecular spacing is less than the equilibrium distance, and the interaction between the molecules is represented by repulsion

(4) $r = r_0$: the molecular spacing is equal to the equilibrium distance, and the resultant force of intermolecular force is zero

The relationship between molecular spacing and interaction force is shown in Figure 1. Under the interaction of molecules, the molecular spacing within a certain range will eventually approach the equilibrium distance.

This process is similar to the car-following interaction between vehicles driving on the road, i.e., the vehicles on the road will finally maintain the distance between their own vehicle and the vehicle in front, taking into account the driving efficiency and safety (hereinafter referred to as required safety distance). Corresponding to the four situations of molecular force, the car-following behavior of a vehicle has the following characteristics:

(1) The longitudinal distance between the two vehicles is beyond the range that affects the decision-making of the driver of the following vehicle, and the speed control of the following vehicle is hardly affected by the leading vehicle.

(2) When the distance between the front and rear vehicles is greater than the required safety distance, the following vehicle actively shortens the following distance to improve driving efficiency.

(3) The distance between the front and rear vehicles is less than the required safety distance. The following vehicle is worried about the risk of collision and slows down to stay away from the leading vehicle.

(4) When the distance between the front and rear vehicles is near the required safety distance, the following vehicle does not actively change the following distance.

Force is the reason to change the motion state of an object. According to the basic idea of building a car-following model based on the characteristics of intermolecular interaction force, the acceleration and deceleration behavior of the vehicle to achieve a suitable following distance is attributed to the "car-following force" of the leading vehicle, which is composed of the "attraction" generated by the driver's pursuit of driving efficiency and the "repulsion" generated by considering driving safety. The edge of the required safety distance between the front and rear of the vehicle is called the demand front and the demand trailing edge, and the force of the following car is shown in Figure 2.

The following behavior of vehicles in a single lane can be compared with the molecules in a long and narrow pipe. When molecules move in a long and narrow pipe, the geometric size on its cross-section allows only one molecule to pass through at a time, and the mass center of the gas molecules in the pipe is always on the line connecting the geometric center of the cross-section of the pipe, as shown in Figure 3. In the figure, f_1 and f_2 are the attractive and repulsive forces between the adjacent molecules, and r is the distance between the centroids of adjacent molecules.

The motion state of molecules in long and narrow pipes is mainly affected by intermolecular interaction and wall potential [11]. The moving adjacent molecules keep a certain distance under the interaction force, which can be simulated by the molecular interaction potential function. The interaction mode of vehicles in a single lane can be simulated by

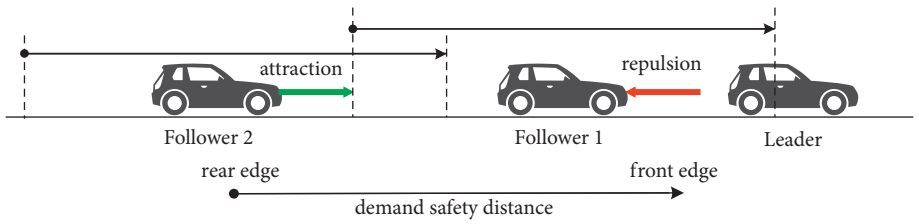

Figure 2: Force status of car-following vehicles.

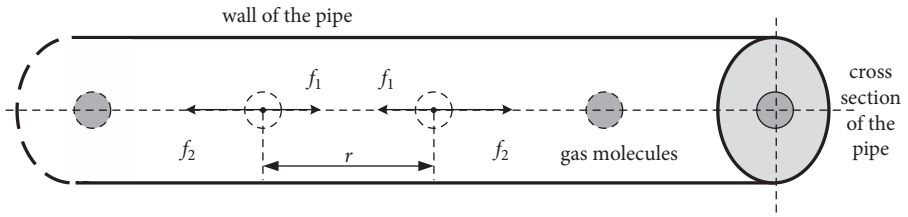

Figure 3: Gas molecules in a long narrow pipe.

the vehicle interaction potential function. Different wall materials, shapes, and other factors make the wall potential produced by the environment in the pipeline different [11–13]. Correspondingly, in the actual vehicle-following behavior, in addition to the interaction between the vehicles, the road environment also affects the motion state of vehicles, which can be simulated by the constructed road avoidance potential function.

Therefore, the thermodynamics of inert gas molecules is similar to the dynamics of the vehicle in the car-following interaction. The research methods and results of inert gas thermodynamics can provide a reference for the study of vehicle interaction and the establishment of a mathematical model. In many studies of fluid molecular thermodynamics, to simulate the interaction mode between microparticles, the introduction of an interaction potential model is of great significance and is widely used in the field of computer simulation. The mathematical expression of interaction potential is called the potential function $\varphi(r)$. Among them, the Lennard–Jones potential [14] is generally applicable to two-body systems, such as inert gases that are dominated by van der Waals force interaction [15].

3. Generalized Lennard–Jones Potential Function

The Lennard–Jones potential model regards the intermolecular potential energy as the combination of the repulsive part and the gravitational part, and as attraction and repulsion are usually related to the reciprocal of the power function of the molecular distance, the basic framework of the potential function is,

$$\varphi(r) = \varphi(r)_{\text{repulsion}} + \varphi(r)_{\text{attraction}} = \frac{A}{r^n} - \frac{B}{r^m}. \tag{1}$$

In the equation, r is the molecular spacing, n and m are the powers of the repulsion term and the attraction term, respectively. m must be greater than n, and A and B are the intermediate variables of the potential function with respect to r. This equation was extensively studied by Ferguson and Kollman [16].

According to the basic relationship between the potential energy of molecules and the distance in molecules thermodynamics, when at the bottom of the potential well, the first derivative of the potential function with respect to r is zero, and its mathematical expression is,

$$\begin{aligned} \varphi(r_e) &= -\varepsilon, \\ \left(\frac{d\varphi}{dr}\right)_{r=r_e} &= 0. \end{aligned} \tag{2}$$

In the equation, ε is the depth of the potential well and r_e is the molecular spacing in the potential well. Substitute equation (1) in equation (2).

$$r_e^{n-m} = \frac{nA}{mB}. \tag{3}$$

Substitute equation (3) back to (1), and get the relationship between the lowest potential energy (potential well depth ε) and the intermediate variables A and B.

$$-\varepsilon = \frac{A}{r_e^n}\left(1 - \frac{n}{m}\right) = \frac{B}{r_e^m}\left(\frac{m}{n} - 1\right). \tag{4}$$

Substitute A and B in equation (4) in equation (1). The generalized Lennard–Jones potential function formula is obtained.

$$\varphi(r) = \frac{\varepsilon}{n-m}\left[m\left(\frac{r_e}{r}\right)^n - n\left(\frac{r_e}{r}\right)^m\right]. \tag{5}$$

When the molecular spacing is in the state of zero potential energy, i.e., substituting $r = \sigma$ in equation (5),

$$\sigma = r_e\left(\frac{m}{n}\right)^{1/n-m}. \tag{6}$$

Upon substituting the above formula in equation (6), we can obtain another form of the generalized Lennard–Jones potential function.

$$\varphi(r) = \frac{\varepsilon}{n-m}\left(\frac{n^n}{m^m}\right)^{1/n-m}\left[\left(\frac{\sigma}{r}\right)^n - \left(\frac{\sigma}{r}\right)^m\right]. \quad (7)$$

The two forms of Lennard–Jones potential are equivalent. Both describe the relationship between the molecular potential energy φ and the molecular spacing r. The difference between the two is that they use different parameters: the former uses the molecular spacing at the bottom of the potential well, and the latter uses the molecular spacing when the potential energy is zero. The Lennard–Jones potential function curve is shown in Figure 4.

In the Lennard–Jones potential model, the interaction force F received by the molecules in the potential field is related to the potential function.

$$F(r) = -\frac{d\varphi}{dr}. \quad (8)$$

Therefore, the two forms of the Lennard–Jones potential function of equations (5) and (7) can be used to obtain two corresponding molecular force expressions.

$$F(r) = \frac{nm\cdot\varepsilon}{n-m}\left(\frac{r_e{}^m}{r^{m+1}} - \frac{r_e{}^n}{r^{n+1}}\right), \quad (9)$$

$$F(r) = \frac{\varepsilon}{n-m}\left(\frac{n^n}{m^m}\right)^{1/n-m}\left(m\frac{\sigma^m}{r^{m+1}} - n\frac{\sigma^n}{r^{n+1}}\right). \quad (10)$$

4. Building of Car-Following Dynamics Model

According to the similarity relationship between the molecular thermodynamics and car-following behavior of vehicles, a vehicle in a single lane can be compared to gas molecules in a long and narrow pipe. Similar to the molecules in long and narrow pipes, the force on the vehicle is attributed to the wall potential and vehicle interaction potential. By analyzing their contributions to the vehicle motion state, a vehicle-following model based on Lennard–Jones potential can be constructed. To apply the model to practice, the parameters in the model need to be calibrated according to the measured data in the actual road environment.

4.1. Vehicle Interaction Potential Function. Through the derivation process of the Lennard–Jones potential function, the mathematical expression of the molecular interaction form is clarified. Combined with the similar characteristics of car-following interaction and molecular interaction, the vehicle interaction potential function can be constructed.

In molecular thermodynamics, because of the magnitude and dispersion of molecules in mass and geometry, the values of m and n are generally 6 and 12, and they usually adopt the form of equation (7), namely the Lennard–Jones 6–12 potential function, referred to as 6–12 potential [17].

$$\varphi_{6-12}(r) = 4\varepsilon\left[\left(\frac{\sigma}{r}\right)^{12} - \left(\frac{\sigma}{r}\right)^6\right]. \quad (11)$$

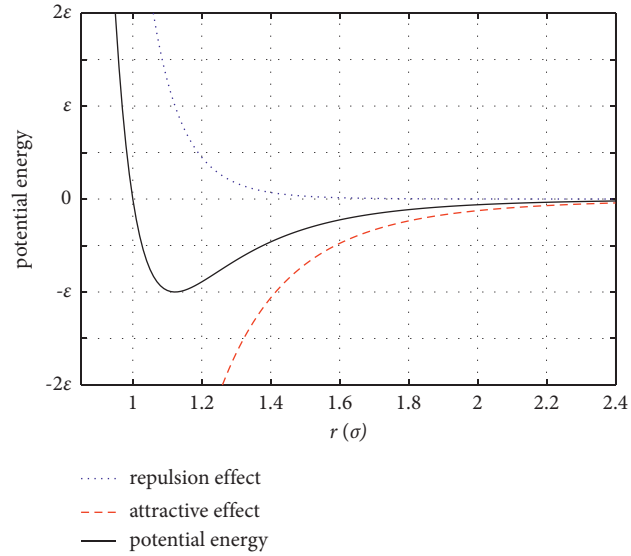

Figure 4: Lennard–Jones potential function.

The 6–12 potential is only a special calibration form of the Lennard–Jones potential, which is a narrow Lennard--Jones potential. The 6–12 potential is a classic pair-potential function in molecular dynamics and thermodynamic modeling. It is also the prototype of the vehicle interaction potential function for building and improving the car-following model based on molecular dynamics in literature [10, 18]. It is built by directly imitating equation (11), directly following the power of the attraction and repulsive terms.

$$\psi_{6-12}(L, X) = 4\varepsilon\left[\left(\frac{X}{L}\right)^{12} - \left(\frac{X}{L}\right)^6\right]. \quad (12)$$

In the equation, L is the distance between the front and rear cars, and X is the immediate demand safe car-following distance of the following cars.

The car-following model built and improved based on the 6–12 potential in the form of equation (12) simulates the actual car-following behavior of the vehicle driving to a certain extent, however, there are two problems, which are as follows:

(1) The calibration of the powers of the attractive and repulsive terms in the Lennard–Jones potential function by the 6–12 potential is based on the characteristics of the microscopic particles in the fluid and their interaction modes. In the scene where a safe following distance is sought in the car-following behavior, the mass, speed, and acceleration of the two interacting bodies, as well as the strength of the interaction and the sensitivity to distance, are very different from the microscopic particles in the fluid. Therefore, the applicability of using the 6–12 potential pair two power calibration method to simulate the interaction between the vehicles is still unclear.

(2) It can be seen from equations (9) and (10) that when the potential energy is 0 (the distance between the

two bodies $r = \sigma$), the resultant force of the interaction is not 0, and when the two bodies are at the bottom of the potential well (when the distance between the two bodies $r = r_e$), the resultant force is 0. Therefore, the vehicle interaction potential function based on equation (7) takes the distance between the two vehicles as the required safety distance when the potential energy is 0, which will cause the force on the rear vehicle not to be 0 when the front and rear vehicles reach the following distance. Even if the required safety distance is reached, the force of the following car is not equal to 0. That is to say, the established and improved car-following model will have certain model errors in simulating the car-following behavior of the vehicle.

Therefore, in view of the above two problems, a car-following model based on the molecular dynamics of the generalized Lennard–Jones potential is presented. Referring to the generalized Lennard–Jones potential function in the form of equation (5), the power n and m of the attraction and repulsive terms are set as the parameters to be calibrated in the model to build the vehicle interaction potential function.

$$\psi(L) = \frac{\varepsilon}{n-m}\left[m\left(\frac{X}{L}\right)^n - n\left(\frac{X}{L}\right)^m\right]. \tag{13}$$

In the formula, ε is the depth of the potential well, X is the required safety distance, L is the actual real-time intervehicle distance, n and m are the powers of attraction and repulsive terms, and n is greater than m.

4.2. Required Safety Distance. The required safety distance for car-following is the distance at which the driver of the following vehicle can immediately brake the vehicle to avoid a collision because of certain emergencies of the current vehicle. Assuming that the immediate speed of the following car is V, the maximum braking acceleration of the following car is d_{Fm}, the immediate speed of the preceding car is V_L, and the maximum braking acceleration of the leading vehicle is d_{Lm}. The sum of the driver's response and the braking trigger time of the vehicle is β, generally 0.5~0.1 s. According to the basic dynamic, the braking distance X_0 of the following vehicle can be obtained as,

$$X_0 = \beta V + \frac{V^2}{2d_{Fm}}. \tag{14}$$

When the following distance has reached the required safe distance and the preceding vehicle is driving at a constant speed or accelerating, if the following vehicle does not accelerate, the following distance will not be lower than the required safe distance in the subsequent driving process. In addition, in actual situations, the safe stopping distance S_0 should also be considered. The safe stopping distance can be several meters to tens of meters depending on conditions, such as different road types. Therefore, the required safety distance when the vehicle in front may suddenly stop moving is,

$$X = S_0 + \beta V + \frac{V^2}{2d_{Fm}}. \tag{15}$$

If the leading vehicle does not suddenly stop moving, when it starts to decelerate, the following vehicle will have collision risk if it does not decelerate in time because the speed is lower than the speed of the following vehicle. The distance X_L traveled by the vehicle in front from the start of braking to stopping is,

$$X_L = \frac{{V_L}^2}{2d_{Lm}}. \tag{16}$$

After the leading vehicle starts to brake, the leading vehicle starts to brake after the time β passes until it stops, and the driving distance of the leading vehicle is,

$$X_F = \beta V_F + \frac{{V_F}^2}{2d_{Fm}}. \tag{17}$$

Considering the safe stopping distance S_0, the required safe distance in this case can be obtained as,

$$X_R = S_0 + \beta V_F + \frac{{V_F}^2}{2d_{Fm}} - \frac{{V_L}^2}{2d_{Lm}}. \tag{18}$$

If the initial state is that the speed of the preceding vehicle is greater than the speed of the following vehicle and if the following vehicle does not accelerate, then the following distance will continue to extend over time. Although this can ensure safe driving, it does not meet the pursuit of driving efficiency for the car behind. The following vehicle will speed up and catch up after detecting that the following distance is greater than the required safety distance. The following distance can only be shortened when it accelerates to a speed greater than the speed of the preceding vehicle. There will be a short-term situation where the speed of the following vehicle is greater than that of the preceding vehicle, and then, the following vehicle will follow the following vehicle will have to slow down until it is at the same speed as the preceding vehicle.

For this scenario, the dynamic analysis of the required safety distance involves complicated elements, including how much acceleration is the leading vehicle chasing, the maximum acceleration value reached, how much deceleration is decelerated, at which stage the preceding car brakes to force the leading vehicle to decelerate, and many more. This analysis process is lengthy, there are many classifications of specific situations, and the actual use of the data set and computing power requirements is relatively large and difficult to use. Therefore, this article will not expand in detail here. In this regard, it has been found in some studies [7] that the relationship between the speed of the front and rear vehicles is an important influencing factor for the following vehicles to actively adjust the speed. Therefore, this paper introduces the influence of the ratio of the speed of the front and rear vehicles based on equations (15) and (18). To simplify and replace the complicated speed change process of the following vehicle in the above scenario, the mathematical expression is,

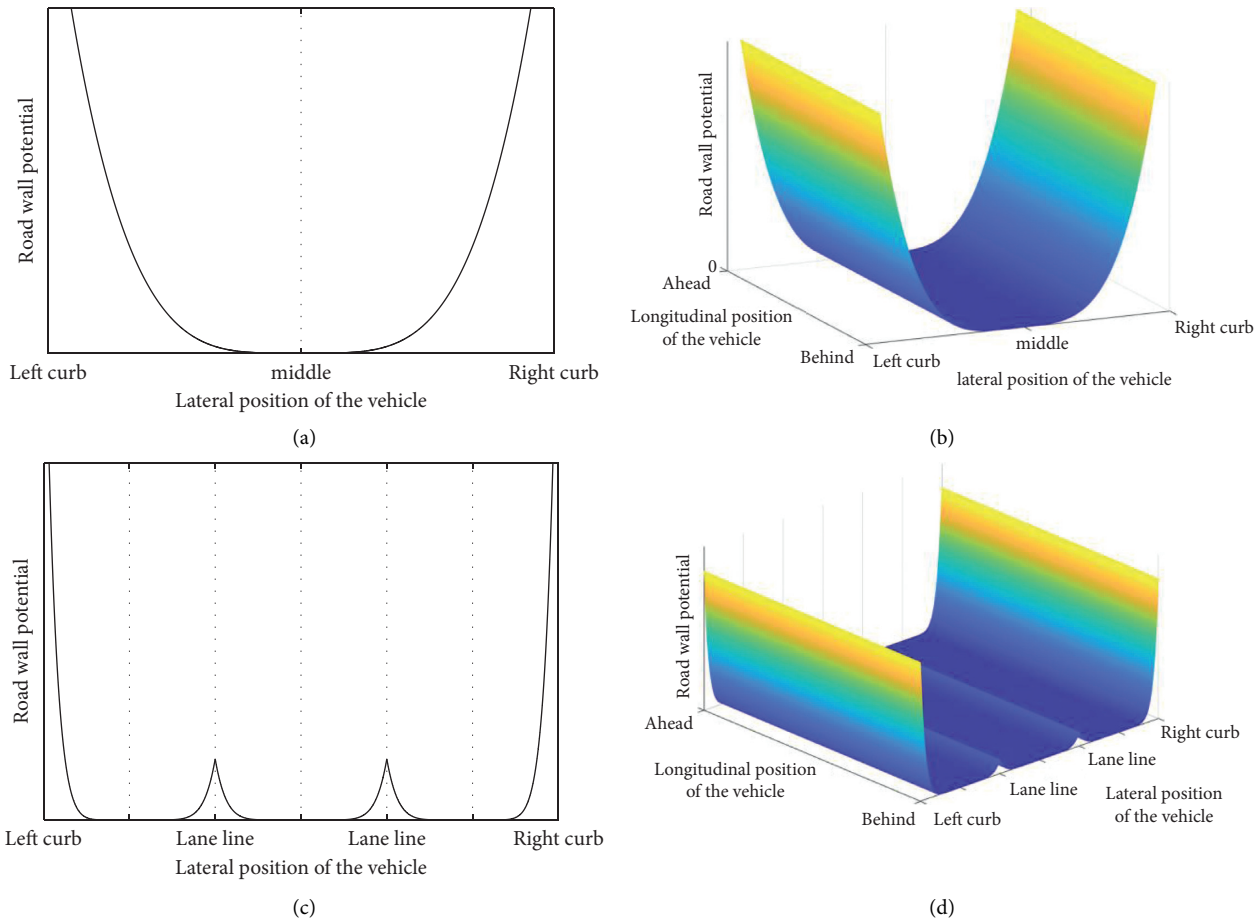

FIGURE 5: Wall potential. (a) Cross-section of road wall potential of single lane. (b) Single lane road wall potential. (c) Cross-section of a 3-lane road wall potential. (d) 3-lane road wall potential.

$$a_j = \lambda_2\left(1 - \frac{V}{V_L}\right). \tag{19}$$

In the formula, a_j is the acceleration because of the speed difference between the front and rear cars, and λ_2 is the parameter for this item.

In this study, to consider the ease of use and rationality of the model, equations (17) and (19) are selected as the basis for model building.

4.3. Road Wall Potential Function. The molecules in a long and narrow pipe are not only constrained by the motion range of the pipe wall but also have a mechanical relationship with the wall so that the molecules will move near the center of the cross-section of the pipe. Vehicles in the lane will also drive in the middle of the lane as much as possible for the reasons of being constrained by traffic regulations and pursuing driving safety.

Therefore, the vehicles in the lane also have a "road wall potential" similar to the wall potential. When there is no interference, the vehicle will preferentially drive in the center of the lane, away from the lane line and the side of the road. Therefore, the potential energy of this potential is the lowest in the center of the lane, a peak occurs at the lane line, and the potential energy is very high near the side of the road. A kind of Gaussian-like potential function model [8] is adopted to construct the road wall potential function:

$$\psi_b = \sum_{i,j} A_i \exp\left(-\frac{\left|d_{V_j}^L\right|^2}{2s^2}\right)\frac{d_{V_j}^L}{\left|d_{V_j}^L\right|}. \tag{20}$$

In the formula, Ψ_b is the potential energy of the road wall, A_i is the potential field strength coefficient of different types of lane boundaries, $d_{V_j}^L$ is the distance vector of the vehicle pointing to the lane boundary, and s is the sensitivity of the vehicle to the lane boundary. Taking single-lane and three-lane roads as examples, the performance of the road wall potential is shown in Figure 5.

4.4. Car-Following Model Based on Mutual Potential Function. The research assumes that the vehicle is not disturbed by other environmental factors and moves longitudinally along the center of the lane. The vehicle is always at the potential well position in the lateral position, and the vehicle acceleration generated by the road wall potential is zero at this time. Therefore, in the study of only the

longitudinal movement of the vehicle following the car, the influence of the road wall potential on the acceleration of the vehicle in the lateral direction of the road can be ignored.

The mathematical analysis of the force of the interaction potential received by the vehicle is the same as the relationship between the equations (5) and (9), i.e., in the vehicle interaction potential field described by the potential function shown in equation (13), the expression of the interaction force received by the vehicle is:

$$F_v(X,L) = \frac{nm\cdot\varepsilon}{n-m}\left(\frac{X^m}{L^{m+1}} - \frac{X^n}{L^{n+1}}\right). \tag{21}$$

The mass of the vehicle is denoted as M, and the simplified model is set to $\lambda_1 = nm\cdot\varepsilon/M(n-m)$. From the basic dynamics' principle, the mathematical expression of acceleration a_i generated by the interaction of the vehicle is,

$$a_i(X,L) = \lambda_1\left(\frac{X^m}{L^{m+1}} - \frac{X^n}{L^{n+1}}\right). \tag{22}$$

Combine equations (19) and (22) to build the generalized Lennard–Jones potential car-following model, referred to as GLM.

$$a_{\mathrm{GLM}} = a_i + a_j = \lambda_1\left(\frac{X^m}{L^{m+1}} - \frac{X^n}{L^{n+1}}\right) + \lambda_2\left(1 - \frac{V}{V_L}\right). \tag{23}$$

5. Model Parameter Calibration

The data of parameter calibration in this study are from the I-80 data set of NGSIM in the United States. The data is collected by the high-altitude camera on the eastbound vehicle trajectory of the I-80 highway in Emeryville, California. It includes the real-time coordinates, speed, and acceleration of the vehicle, which can provide a sufficient data basis for the car-following model [19].

Genetic algorithm is a search algorithm for solving optimization problems, which was proposed by Bagley [20]. The genetic algorithm imitates the principles of genetics, transforms the mathematical problem to be solved into the initial population, and continuously approaches the optimal solution in the process of multiple "gene exchanges" and iterations. The basic steps are shown in Figure 6.

50 groups of vehicle movement data with obvious car-following relationship and continuous car-following time of more than 45 s are selected from the data set. The safe stopping distance is taken as 2 m, and the driver's response time is taken as 0.7 s. According to the genetic algorithm described in the literature [19], the selection method in this paper is the roulette selection method, using the uniform crossover method, and the mutation rate is 0.01. The total number of data samples is 6,154, and the parameter calibration results are shown in Table 1.

6. Model Evaluation

To reasonably evaluate the GLM, the improved molecular car-following model (referred to as the M-MD car-following model) and the intelligent driver model (IDM) described in the literature [18] are selected for comparison, and the parameters are adjusted and calibrated according to the collection scene of the same data set as above.

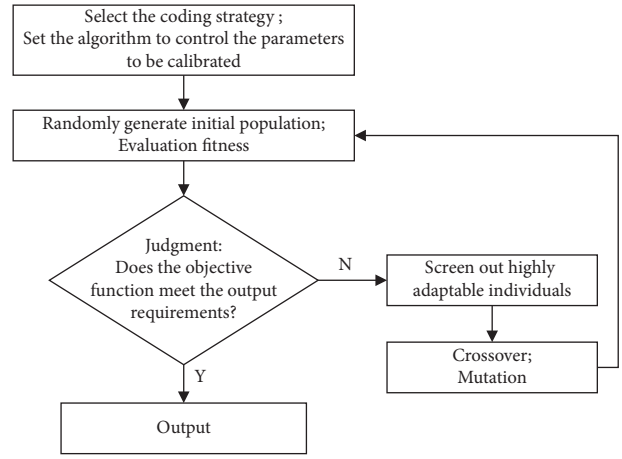

Figure 6: Basic steps of genetic algorithm.

Table 1: Result of parameter calibration of GLM.

Parameters	Calibration values
M	0.7103
N	1.6754
λ_1	29.2322
λ_2	44.4901

The formula of the M-MD car-following model is,

$$a_{M-\mathrm{MD}} = \lambda_1\left(2\frac{X_n^{\,6}}{L^7} - \frac{1}{L}\right)\left(\frac{X_n}{L}\right)^6 + \lambda_2\left(1 - \frac{V_n}{V_{n+1}}\right). \tag{24}$$

In the formula, $a_{\mathrm{M\text{-}MD}}$ is the acceleration of the leading vehicle, X_n is the required safety distance, L is the instantaneous distance following the car, and V_n and V_{n+1} are the instantaneous speeds of the leading vehicle and the preceding car, respectively. The parameter calibration results of the M-MD model are shown in Table 2.

IDM was proposed by Treiber et al. [21] in 2000 and is widely used in the theory and simulation of manual driving vehicle-following model [22, 23]. The formula of IDM car-following model is,

$$a_n = a\left[1 - \left(\frac{v_n}{v_0}\right)^4 - \left(\frac{S_0 + v_nT - v_n(v_{n-1} - v_n)/2\sqrt{ab}}{L}\right)^2\right]. \tag{25}$$

In the formula, a_n is the acceleration of vehicle n, v_n and v_{n-1} are the instantaneous speeds of vehicle n and vehicle $n-1$, v_0 is the free flow velocity, L is the following distance, T is the safe following time interval, S_0 is the safety stopping distance, a is the maximum acceleration parameter of the vehicle, and b is the comfortable deceleration. The parameter calibration results of IDM are shown in Table 3.

Table 2: Result of parameter calibration of M-MD model.

Driving state	λ_1	λ_2
Regular driving	1.3401	9.4095
Accelerating	0.9548	17.3827
Braking	66.5029	0.0141

Table 3: Result of parameter calibration of IDM.

Parameters	Calibration values
A	1 m/s^2
B	2 m/s^2
v_0	33.3 m/s
s_0	10 m
T	1.5 s

Three sets of data are extracted from the data set and simulated in MATLAB to obtain the time-trajectory figure and time-acceleration curve image of the actual measurement of the follower car and the output of the three models.

The measured data of the preceding and following cars and the output time-trajectory of the model simulation are shown in Figure 7:

Through the comparison of the output time-trajectory figure, it is found that the M-MD model will suddenly and sharply accelerate and decelerate abnormally. Through mathematical analysis, it is found that the main reason is that the power of the attraction and repulsive terms in the model is too large, which makes it too sensitive to the following distance. GLM model reasonably sets the power of the two terms according to the actual situation, so both GLM model and IDM model show more reasonable simulation results.

After excluding the abnormal acceleration data of the M-MD, the actual acceleration value of the leading vehicle and the time-acceleration output by the model simulation are shown in Figure 8:

By the comparison of the output time-space trajectory diagrams, it is found that the acceleration change trend output by the M-MD model and GLM has a better fit with the measured value, while the curve output by IDM is smoother.

To compare and evaluate the accuracy of the model more intuitively, the mean absolute error (MAE) and root mean square error (RMSE) are introduced to evaluate the accuracy of the model.

$$\begin{aligned} \mathrm{MAE} &= \frac{1}{N}\sum_{i=1}^{N}\left|y_i - \widehat{y}_i\right|, \\ \mathrm{RMSE} &= \sqrt{\frac{1}{N}\sum_{i=1}^{N}\left(y_i - \widehat{y}_i\right)^2}. \end{aligned} \tag{26}$$

In the formula, N is the sample size, y_i is the measured value, and $\widehat{y}_i$ is the estimated value output by the model. The lower the MAE value and RMSE value, the smaller the model estimation error, and the higher the model accuracy. Compare the error between the output acceleration of the three models and the measured data with 1867 samples in the data set. The results are shown in Table 4.

The comparison results of the model errors show that GLM has higher accuracy than IDM, and the accuracy of both is significantly better than the M-MD model. The mathematical form of GLM built in this paper can abandon the way of grouping and calibrating the parameters of the M-MD model in the three conditions of acceleration, uniform speed, and deceleration. It is simpler and more efficient when in use.

7. Model Stability

The stability of the car-following model reflects whether the stable traffic flow simulated by the model can restore stability again after being stimulated. To test the stability of the GLM model, MATLAB is used to build a simulation environment for testing.

The simulation content is as follows: a fleet of 20 vehicles is in the longitudinal direction, the fleet runs at a constant speed, and the adjacent vehicles maintain the required safe following distance at this speed. Test the development trend of the fleet movement state under the sudden acceleration and deceleration of the foremost leading vehicle, respectively.

The initial speed of the model fleet is 12 m/s, and the leading vehicle is reduced and accelerated by 1 m/s^2 for 2 seconds. A total of 10 seconds is simulated, and the simulation step is 1 ms. The simulation result is shown in Figure 9.

The simulation results show that after being disturbed by the front, the simulation fleet shows the characteristics of acceleration fluctuation propagating from front to back with time and gradual attenuation of intensity, which is consistent with the performance of the fleet in the actual situation. When the turbulence of the traffic flow reaches the end of the fleet, the acceleration of the vehicles in the simulation fleet approaches zero again, and the stable running state is restored within a short time after being disturbed. Therefore, it can be considered that GLM has good stability when faced with disturbances.

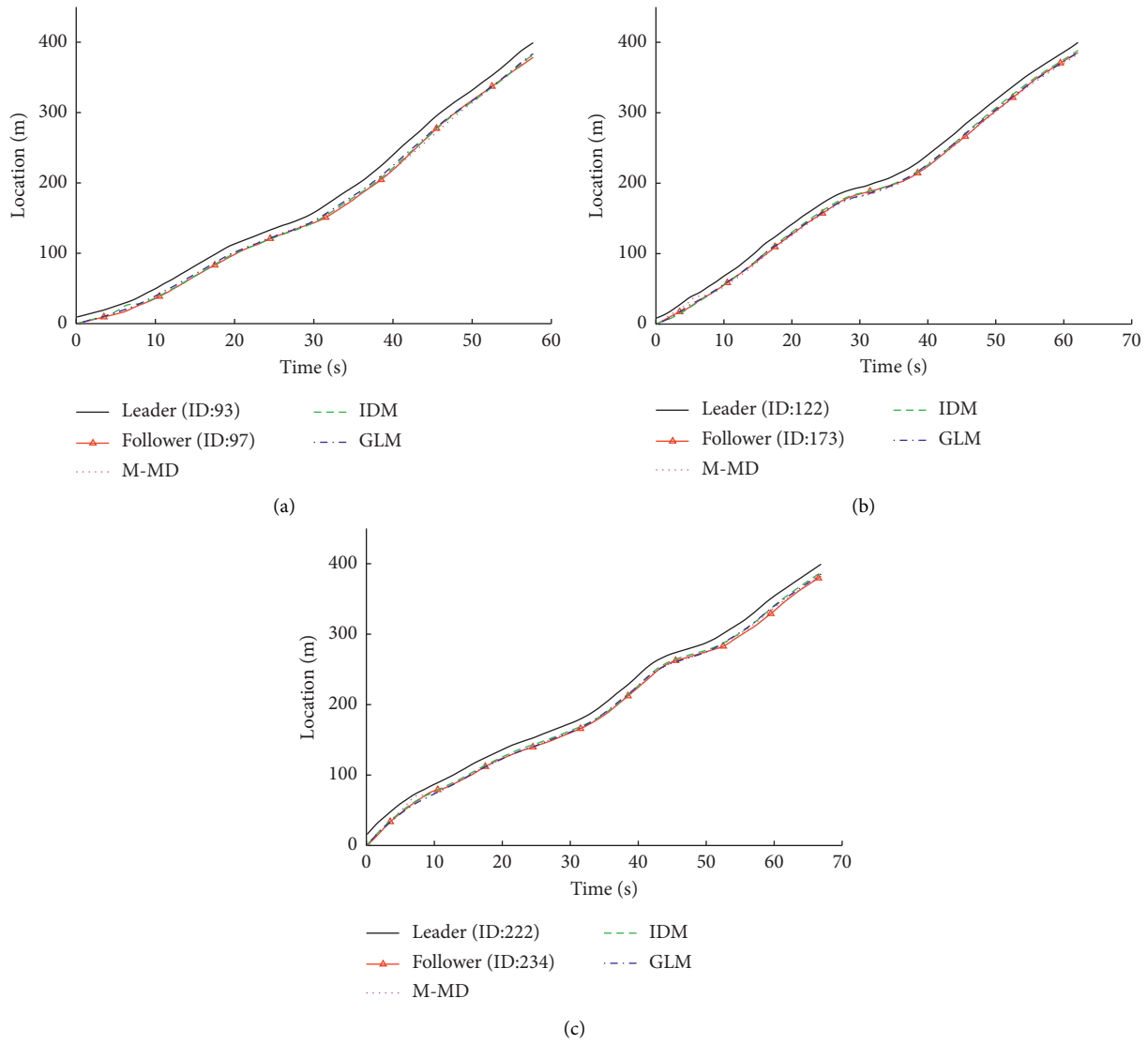

Figure 7: Time-trajectory curves of model simulation. (a) Vehicle 97 follow vehicle 93. (b) Vehicle 173 follow vehicle 122. (c) Vehicle 234 follow vehicle 222.

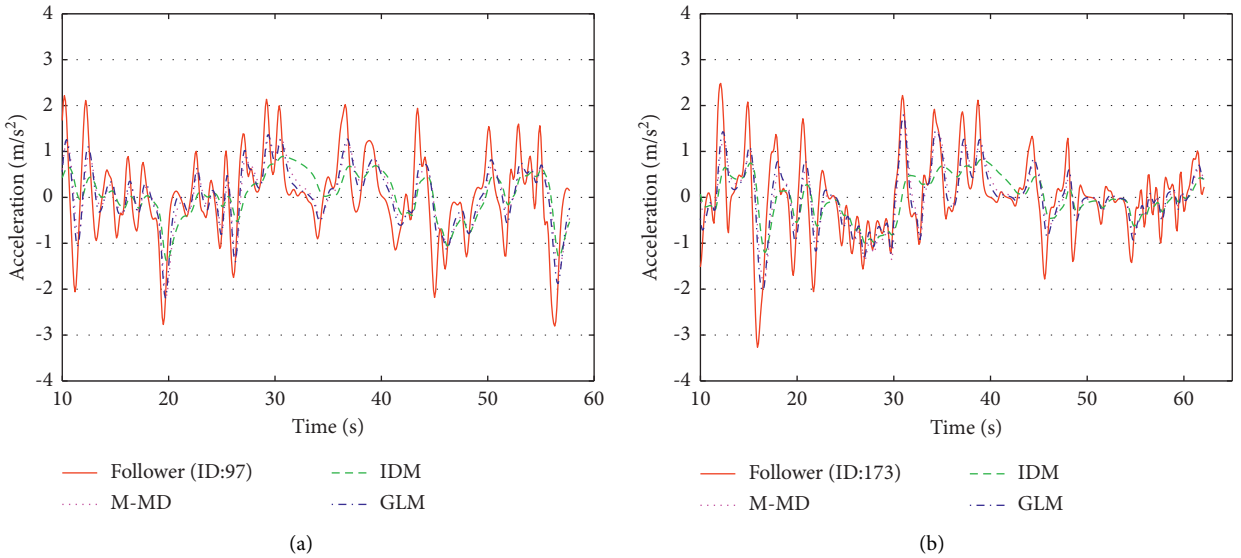

Figure 8: Continued.

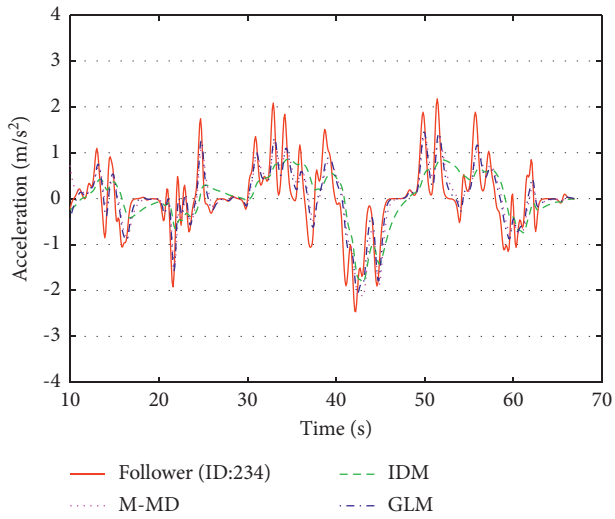

(c)

Figure 8: Time-acceleration curves of model simulation. (a) Vehicle 97 follow vehicle 93. (b) Vehicle 173 follow vehicle 122. (c) Vehicle 234 follow vehicle 222.

Table 4: Models error comparison.

Models	MAE	RMSE
M-MD	1.4867	0.7473
IDM	0.8004	0.5982
GLM	0.3772	0.5240

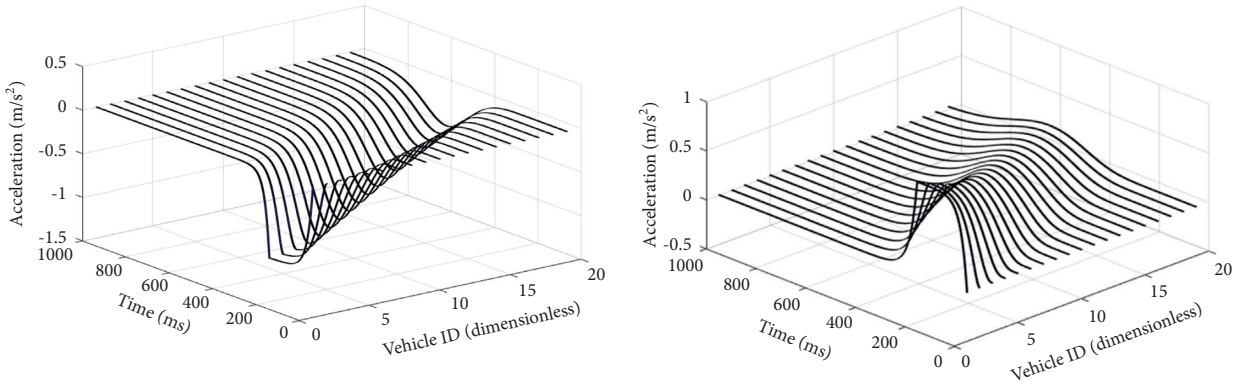

(a) (b)

Figure 9: Time-acceleration figure obtained from model simulation. (a) The leader of the simulation fleet is disturbed by deceleration. (b) The leader of the simulation fleet is disturbed by acceleration.

8. Conclusion

Certain thermodynamic properties of microscopic particles in certain fluids are similar to the car-following behavior of vehicles on the road. The complex car-following behavior is simplified as the process of the rear car constantly looking for the required safe distance. Combining the Lennard–Jones potential model of molecular thermodynamics with the actual situation of vehicles in road traffic, many similar characteristics between the safe following distance and the equilibrium distance of microscopic fluid particles are explained.

The narrow and long molecular pipeline is used to compare the car-following environment of a single lane, and the factors affecting the vehicle's motion state in the road environment are analyzed. The complicated car-following behavior is simplified as the process of continuously searching for the required safety distance by the leading vehicle. By analyzing the mathematical derivation process of the Lennard–Jones potential function, referring to the parameter variable relationship of the interaction potential function of inert gas molecules, avoiding the problems existing in the existing car-following model based on

molecular dynamics, establishing the vehicle interaction potential function, and considering the influence of lane boundary on the transverse position of vehicles on the road, a car following model based on Lennard–Jones potential is proposed.

Compared with the simulation test results of other models, the model has good accuracy and stability and can effectively reflect the motion of vehicles. It has reference significance for the study of traffic flow characteristics and road traffic safety. It also lays a theoretical foundation for the research on the decision-making behavior of complex driving [24, 25].

Data Availability

The NGSIM dataset used in this paper can be downloaded from the website https://data.transportation.gov/Automobiles/Next-Generation-Simulation-NGSIM-Vehicle-Trajector/8ect-6jqj.

Conflicts of Interest

The authors declare that they have no conflicts of interest.

References

[1] D. C. Gazis, R. Herman, and R. W. Rothery, "Nonlinear follow-the-leader models of traffic flow," *Operations Research*, vol. 9, no. 4, pp. 545–567, 1961.

[2] M. Bando, K. Hasebe, A. Nakayama, A. Shibata, and Y. Sugiyama, "Dynamical model of traffic congestion and numerical simulation," *Physical Review E*, vol. 51, no. 2, pp. 1035–1042, 1995.

[3] D. Helbing and B. Tilch, "Generalized force model of traffic dynamics," *Physical Review E*, vol. 58, no. 1, pp. 133–138, 1998.

[4] R. Jiang, Q. S. Wu, and Z. J. Zhu, "Full velocity difference model for a car-following theory," *Physical Review E - Statistical, Nonlinear and Soft Matter Physics*, vol. 64, no. 1-2, Article ID 017101, 2001.

[5] X. Chen, *A Study on Vehicle Operating Safety Characteristics Based on Molecular Dynamics*, Jilin University, China, Jilin, (in Chinese), 2013.

[6] D. Qu, J. Yang, X. Chen, and X. Bian, "Molecular kinetics behavior of car-following and its model," *Journal of Jilin University (Engineering and Technology Edition)*, vol. 42, no. 05, pp. 1198–1202, 2012, (in Chinese).

[7] M. T. Wolf and J. W. Burdick, "Artificial potential functions for highway driving with collision avoidance," in *Proceedings of the 2008 IEEE International Conference on Robotics and Automation*, pp. 3731–3736, IEEE, Pasadena, CA, USA, May 2008.

[8] L. Li, J. Gan, Q. U. Xu, P. Mao, and B. Ran, "Car-following model based on safety potential field theory under connected and automated vehicle environment," *China Journal of Highway and Transport*, vol. 32, no. 12, pp. 76–87, 2019, (in Chinese).

[9] J. Li, D. Qu, C. Liu, W. Wang, and D. Liu, "Car-following characteristics and its models based on molecular dynamics," *Journal of Highway and Transportation Research and Development*, vol. 35, no. 03, pp. 126–131, 2018, (in Chinese).

[10] L. Yang, H. Wang, L. I. Shuai, and X. Qiu, "Improved molecular dynamics car-following model," *Journal of Chongqing University*, vol. 44, no. 7, pp. 26–33, 2021, (in Chinese).

[11] B. Cao, M. Chen, and Z. Guo, "Molecular dynamics studies of slip flow in nanochannel," *Journal of Engineering and Thermophysics*, vol. 24, no. 04, pp. 670–672, 2003, (in Chinese).

[12] G. Mie, "Zur kinetischen Theorie der einatomigen Körper," *Annalen der Physik*, vol. 316, no. 8, pp. 657–697, 1903.

[13] M. Tohidi and D. Toghraie, "The effect of geometrical parameters, roughness and the number of nanoparticles on the self-diffusion coefficient in Couette flow in a nanochannel by using of molecular dynamics simulation," *Physica B: Condensed Matter*, vol. 518, pp. 20–32, 2017.

[14] H. Rahmatipour, A.-R. Azimian, and O. Atlaschian, "Study of fluid flow behavior in smooth and rough nanochannels through oscillatory wall by molecular dynamics simulation," *Physica A: Statistical Mechanics and Its Applications*, vol. 465, pp. 159–174, 2017.

[15] R. S. Voronov, D. V. Papavassiliou, and L. L. Lee, "Slip length and contact angle over hydrophobic surfaces," *Chemical Physics Letters*, vol. 441, no. 4-6, pp. 273–276, 2007.

[16] D. M. Ferguson and P. A. Kollman, "Can the Lennard-Jones 6-12 function replace the 10-12 form in molecular mechanics calculations?" *Journal of Computational Chemistry*, vol. 12, no. 5, pp. 620–626, 1991.

[17] T. Wang, Z. Gao, and X. Zhao, "Multiple velocity difference model and its stability analysis," *Acta Physica Sinica*, vol. 55, no. 02, pp. 634–640, 2006, (in Chinese).

[18] J. E. Lennard-Jones, "Cohesion," *Proceedings of the Physical Society*, vol. 43, no. 5, pp. 461–482, 1931.

[19] Y. Luo, D. Yuan, and G. Tang, "Hybrid Genetic Algorithm for solving systems of nonlinear equations," *Chinese Journal of Computational Mechanics*, vol. 22, no. 01, pp. 109–114, 2005, (in Chinese).

[20] J. D. Bagley, *The Behavior of Adaptive Systems which Employ Genetic and Correlation Algorithms*, University of Michigan, Ann Arbor, MI, USA, 1967.

[21] M. Treiber, A. Hennecke, and D. Helbing, "Congested traffic states in empirical observations and microscopic simulations," *Physical review E*, vol. 62, no. 2, pp. 1805–1824, 2000.

[22] M. Zhu, X. Wang, A. Tarko, and S. e. Fang, "Modeling car-following behavior on urban expressways in Shanghai: a naturalistic driving study," *Transportation Research Part C: Emerging Technologies*, vol. 93, pp. 425–445, 2018.

[23] M. Zhu, X. Wang, and Y. Wang, "Human-like autonomous car-following model with deep reinforcement learning," *Transportation Research Part C: Emerging Technologies*, vol. 97, pp. 348–368, 2018.

[24] X. Wang, S. Ramírez-Hinestrosa, J. Dobnikar, and D. Frenkel, "The Lennard-Jones potential: when (not) to use it," *Physical Chemistry Chemical Physics*, vol. 22, no. 19, pp. 10624–10633, 2020.

[25] B. Lu, *Modeling and Analysis of Car-Following Behavior Using Data-Driven Methods*, Southwest Jiaotong University, Sichuan, China, (in Chinese), 2017.